Analysis of non-stationary temperature field generated by a shaftless screw conveyor heated by Joule–Lenz effect

Stanisław Ledakowicz, Olexa Piddubniak

Faculty of Process and Environmental Engineering, Lodz University of Technology,
Wolczanska St. 215, 90-924 Lodz, Poland

The non-stationary problem of temperature distribution in a circular cylindrical channel of infinite length filled with a homogeneous biomass material moving with a constant velocity in the axial direction was investigated. The heat source was a shaftless helical screw (or auger), which was heated with an electric current due to the Joule–Lenz effect and rotated uniformly around the axis of symmetry of the channel. Similar problems arise in the thermal processing of biomaterials using screw conveyor in pyrolysis and mass sterilization and pasteurization of food products. The problem is solved using the expansion of given and required functions in Fourier series over angular coordinate and integral Fourier and Laplace transforms over axial coordinate and time, respectively. As a result, the temperature field is obtained as the sum of two components, one of which, global, is proportional to time, and the other, which forms the microstructure of the temperature profile, is given by Fourier–Bessel series. The coefficients of the series are determined by the integrals calculated using the Romberg method. Based on the numerical calculations, the analysis of the space-time microstructure of the temperature field in the canal was performed. A significant dependence of the features of this microstructure on the geometric, kinematic and thermodynamic characteristics of the filling biomass and the screw was revealed.

Keywords: screw reactor, rotating shaftless screw, electric heating, non-stationary temperature field, analytico-numerical method

1. INTRODUCTION

In recent years, theoretical and experimental studies of pyrolysis of various raw materials, including biomass and waste, have been intensified (Guda et al., 2015). At the same time, screw reactors (or auger reactors) are attracting more and more attention in the scientific literature. These reactors are attractive for their versatility in transforming biomass wastes, and have been recognized as one of the best technologies for slow or intermediate pyrolysis, but they have also become one of the most popular and commercially available methods. A comprehensive assessment of screw systems, their advantages and disadvantages, along with historical aspects of the development of such technical equipment has recently been presented in a broad literature review by Campuzano et al. (2019).

As is known, raw material is fed into a heated reactor and transported by a rotating screw. In addition to transportation, appropriately designed screws, improving the contact between the particles of the trans-

www.czasopisma.pan.pl   PAN   www.journals.pan.pl

S. Ledakowicz, O. Piddubniak, Chem. Process Eng., 2021, 42 (2), 119–137

ported mass and the heated surface, are able to enhance the mixing of particles and heat transfer between solid coolants and reagents (Aramideh et al., 2015), and ensuring the optimal duration of the feedstock in the reactor under appropriate thermal conditions also promote pyrolysis (]Nachenius et. al., 2015). It is also known that pyrolysis is an endothermic process that requires the addition of heat not only to increase the temperature of the reagents to the pyrolysis temperature, but also to stimulate chemical reactions of pyrolysis, i.e. enthalpy for pyrolysis (Martínez et al., 2013). The supply of thermal energy required for pyrolysis in single- or twin-screw reactors is achieved by indirect heating through the walls of the reactor, through the surface of the screw, or by direct heating using heat carriers. Herewith the heating temperature should be slightly higher than the required pyrolysis temperature. Thus, one of the important issues in the design of screw reactors is to create such a distribution of the temperature field in them, which would contribute to the efficient performance of the pyrolysis process (Yang et al., 2013). Moreover, as the scale of the reactor increases, heat transfer becomes a primary problem for improving the efficiency of the pyrolysis process, especially fast pyrolysis. In this regard, Ledakowicz et al. (2019) based on extensive experiments showed, using a pyrolyzer with an electrically heated screw, the principle which was described by Lepez and Sajet (2009) in their patent, that the pyrolysis temperature has a great influence on the product yield and product properties.

A typical screw reactor consists of a fixed outer shell and a screw that rotates around a central, sometimes empty shaft. The geometry of the screw flight is one of the main features, which is modified depending on the application (transportation, feeding, mixing or their combination) and process requirements. In industrial applications both shafted and shaftless screw systems are used (Biogreen, 2016; ETIA S.A.S., 2019). This type of screw, heated by the Joule effect, is used for pyrolysis of viscous, gummy or sticky substances and mass sterilization and pasteurization of food products (THERMOFLO Equipment Company, 2018).

Along with experimental research, mathematical modeling of processes in screw reactors occupies an important place. Thus, in the works of Shi et al. (2019a and 2019b) using numerical hydromechanics methods (see e.g., Kovacevic et al., 2007), the distribution of velocities of a multiphase liquid in a screw reactor was simulated, and the axial temperature distribution was also determined (Nachenius et al., 2015). Nevertheless, the problem of the analytical description of the temperature field distribution in the reactor, its dependence on the geometric, mechanical and thermodynamic parameters of the systems, remains important.

In this paper, an attempt is made to mathematically model the temperature field in a circular heat-insulated channel filled with a mobile medium such as homogeneous biomass material, assuming that the main heat in the reactor comes from a rotating shaftless screw due to the Joule–Lenz effect. It is necessary to perform an analysis of the temperature in the channel depending on the spatial coordinates and time, the geometric dimensions of the screw and the angular velocity of its rotation, the thermodynamic parameters of the substance filling the channel and the speed of its movement.

2. STATEMENT OF THE PROBLEM AND SOLUTION METHOD

Consider an infinitely long channel of circular cross section with radius R_1, containing e.g. homogeneous biomass that moves in the axial direction with a uniform distribution of linear velocities v_0. Biomass is heated due to the action of a heat source in the form of a screw of finite width, which rotates around the axis of symmetry of the channel with an angular velocity ω. The screw, in turn, is heated by a pulsed electric current of force I, uniformly distributed over its surface. Assume also that the channel surface is thermally insulated. Then to find the temperature field in the channel it is necessary to solve the nonstationary

inhomogeneous equation of thermal conductivity (Luikov, 1968; Carslaw and Jaeger, 1959)

$$c_p \rho \left(\frac{\partial T}{\partial \tau} + v_0 \frac{\partial T}{\partial z} \right) = \lambda \left[\frac{1}{r} \frac{\partial}{\partial r} \left(r \frac{\partial T}{\partial r} \right) + \frac{1}{r^2} \frac{\partial^2 T}{\partial \theta^2} + \frac{\partial^2 T}{\partial z^2} \right] + q\,(r, \theta, z, \tau) \tag{1}$$

$$(0 < r < R_1, 0 < \theta < 2\pi, -\infty < z < \infty, \tau > 0)$$

under the initial condition

$$T|_{\tau=0} = T_0 \tag{2}$$

the condition of thermal insulation on the surface of the channel

$$\frac{\partial T}{\partial r}\bigg|_{r=R_1} = 0 \tag{3}$$

and the condition of boundedness of a solution of the problem on the axis of the channel

$$\frac{\partial T}{\partial r}\bigg|_{r=0} = 0 \tag{4}$$

Here ρ is the density of the moving biomass, c_p is its heat capacity at constant pressure; λ is the coefficient of thermal conductivity; r, θ, z – the cylindrical coordinate system with origin on the axis of the circular channel; τ is the time.

Replacing screw by a system of continuously distributed heat sources, the intensity function of the heat source $q(r, \theta, z, \tau)$ is written in the form

$$q(r, \theta, z, \tau) = \frac{q_0 \varepsilon}{\varepsilon - \varepsilon_0} r \left[H(r - R_2) - H(r - R_0) \right] \sum_{m=-\infty}^{\infty} \delta \left[(\theta + 2\pi m + \omega \tau) r \cos \varphi_0 - z \sin \varphi_0 \right] H(\tau) \tag{5}$$

where $H(x)$ is the Heaviside function, $\delta(x)$ is the Dirac function, $q_0 = \rho_0 j^2$; ρ_0 is the specific electrical resistance of the conductor; $j = I/S$ is the electric current density of a conductor, $I = \text{const.}$; $S = h \times h_1$ is the cross-sectional area of the screw, h is its thickness and $h_1 = R_0 - R_2$ is its width; R_0 and R_2 are the radii of the edges of the screw equidistant to the surface of the cylindrical channel, $0 < R_2 < R_0 < R_1$; $\varepsilon = R_0/R_1$, $\varepsilon_0 = R_2/R_1$; φ_0 is the angle of rise of the edges of the screw to the axis of the channel $0z$ (Fig. 1; here, the upper figure is for the spiral only, and the lower figures are for the entire system).

It is convenient to use a substitute to solve the problem (Smirnov, 1964)

$$T(r, \theta, z, \tau) - T_0 = U(r, \theta, z, \tau)e^{bz} \tag{6}$$

Then, if $b = v_0/(2a)$, where a is the coefficient of thermal diffusivity of biomass, $a = \lambda/(c_p \rho)$, from Eq. (1) we obtain the differential equation

$$\frac{1}{a} \frac{\partial U}{\partial \tau} - \left[\frac{1}{r} \frac{\partial}{\partial r} \left(r \frac{\partial U}{\partial r} \right) + \frac{1}{r^2} \frac{\partial^2 U}{\partial \theta^2} + \frac{\partial^2 U}{\partial z^2} - b^2 U \right] = \frac{1}{\lambda} e^{-bz} q(r, \theta, z, \tau)$$

$$(0 < r < R_1, \ \ 0 < \theta < 2\pi, \ \ -\infty < z < \infty, \ \ \tau > 0) \tag{7}$$

with appropriate initial and boundary conditions

$$U|_{\tau=0} = 0 \tag{8}$$

$$\frac{\partial U}{\partial r}\bigg|_{r=R_1} = 0 \tag{9}$$

$$\frac{\partial U}{\partial r}\bigg|_{r=0} = 0 \tag{10}$$

www.czasopisma.pan.pl   PAN   www.journals.pan.pl

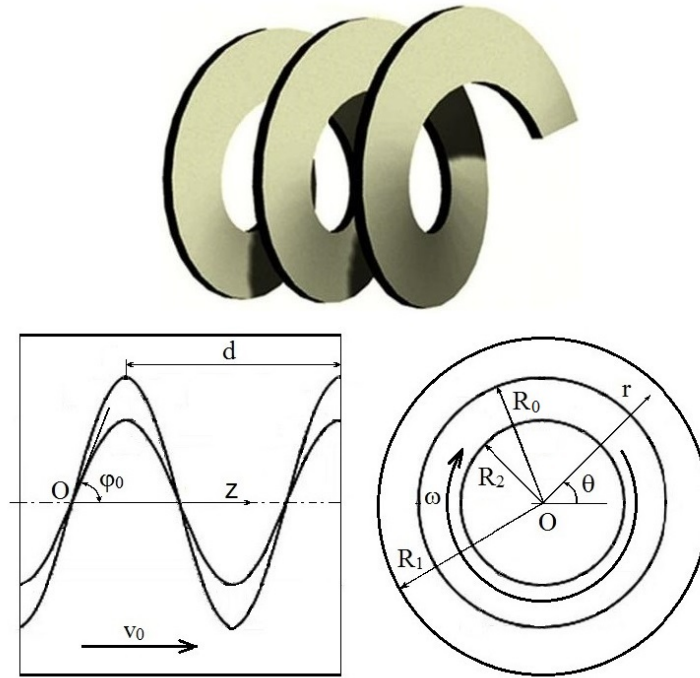*S. Ledakowicz, O. Piddubniak,   Chem. Process Eng., 2021, 42 (2), 119–137*

Fig. 1. View of the shaftless screw and the dimensions of its sectional flight

Let us represent the functions $U(r, \theta, z, \tau)$ and $q(r, \theta, z, \tau)$ in the form of Fourier series (Korn and Korn, 2000)

$$U(r, \theta, z, \tau) = \sum_{m=-\infty}^{\infty} U_m(r, z, \tau) e^{-im\theta} \quad (0 < \theta < 2\pi) \tag{11}$$

$$q(r, \theta, z, \tau) = \sum_{m=-\infty}^{\infty} q_m(r, z, \tau) e^{-im\theta} \quad (0 < \theta < 2\pi) \tag{12}$$

where for the expansion coefficients there are formulae:

$$
\begin{aligned}
U_m(r, z, \tau) &= \frac{1}{2\pi} \int_0^{2\pi} U(r, z, \theta, \tau) e^{im\theta} \, \mathrm{d}\theta \\
q_m(r, z, \tau) &= \frac{1}{2\pi} \int_0^{2\pi} q(r, z, \theta, \tau) e^{im\theta} \, \mathrm{d}\theta
\end{aligned}
\tag{13}
$$

We also apply to Eqs. (7)–(10) the integral Fourier transform over z and the integral Laplace transform over τ (Korn and Korn, 2000). Then we obtain the following boundary value problem:

$$\left[\frac{\mathrm{d}^2}{\mathrm{d}r^2} + \frac{1}{r} \frac{\mathrm{d}}{\mathrm{d}r} - \left(\frac{m^2}{r^2} + s^2 \right) \right] U_m^{FL}(r, k, p) + Q_m^{FL}(r, k, p) = 0 \quad (0 < r < R_1) \tag{14}$$

$$\left. \frac{\mathrm{d}U_m^{FL}}{\mathrm{d}r} \right|_{r=R_1} = 0 \tag{15}$$

$$\left. \frac{\mathrm{d}U_m^{FL}}{\mathrm{d}r} \right|_{r=0} = 0 \tag{16}$$

Here

$$U_m^{FL}(r, k, p) = \int\limits_{-\infty}^{\infty} e^{-ikz}\,dz \int\limits_{0}^{\infty} U_m(r, z, \tau)e^{-p\tau}\,d\tau$$

$$Q_m^{FL}(r, k, p) = \int\limits_{-\infty}^{\infty} e^{-ikz}\,dz \int\limits_{0}^{\infty} Q_m(r, z, \tau)e^{-p\tau}\,d\tau \quad (-\infty < k < \infty, \ Re\,p > 0)$$

(17)

are the Fourier transform over z and the integral Laplace transform over τ of the functions $U_m(r, z, \tau)$ and $Q_m(r, z, \tau)$, where

$$Q_m(r, z, \tau) = \lambda^{-1} q_m(r, z, \tau)e^{-bz} \tag{18}$$

and also

$$s = \sqrt{k^2 + b^2 + \frac{p}{a}} \quad (I_m s \geq 0) \tag{19}$$

Solving the boundary value problem (14)–(16) (Korn and Korn, 2000), we obtain

$$U_m^{FL}(r, k, p) = \int\limits_{0}^{r} D_m^{FL}(r, r', k, p)Q_m^{FL}(r', k, p)r'\,dr' +$$

$$+ \int\limits_{r}^{R_1} D_m^{FL}(r, r', k, p)Q_m^{FL}(r', k, p)r'\,dr' \quad (0 < r < R_1),$$

(20)

where

$$D_m^{FL}(r, r', k, p) = \frac{I_m(sr')}{I_m'(sR_1)} S_m(sR_1, sr) \tag{21}$$

$$S_m(sx, sy) = I_m'(sx)K_m(sy) - K_m'(sx)I_m(sy) \tag{22}$$

Here $I_m(x)$ is the modified Bessel function of the m-th order; $K_m(x)$ is the McDonald function of the m-th order; the prime symbol marked the derivatives of these functions.

Returning now in Eq. (20) to the field of originals, we obtain a representation for $U_m(r, z, \tau)$ in the form of convolution integrals

$$U_m(r, z, \tau) = \int\limits_{0}^{r} r'\,dr' \int\limits_{-\infty}^{\infty} dz' \int\limits_{0}^{\tau} D_m(r, r', z', \tau')Q_m(r', z - z', \tau - \tau')\,d\tau' +$$

$$+ \int\limits_{r}^{R_1} r'\,dr' \int\limits_{-\infty}^{\infty} dz' \int\limits_{0}^{\tau} D_m(r', r, z', \tau')Q_m(r', z - z', \tau - \tau')\,d\tau' \quad (0 < r < R_1)$$

(23)

The analysis of the function $D_m^{FL}(r, r', k, p)$, based on the asymptotic behavior of cylindrical functions for small arguments sx and sy (Abramowitz and Stegun, 1972), shows that for $m = 0$ this function has a pole at the point $s^2 = 0$, i.e., at the point $p = p_0 = -a(k^2 + b^2)$. At the same time, for arbitrary m, this function has poles that coincide with the zeros of the function $I_m'(sR_1)$. If we take into account that $I_m(x) = e^{-i\pi m/2} J_m(ix)$, where $J_m(y)$ is the Bessel function of the m-th order, then the zeros of function $I_m'(sR_1)$ will be determined by the zeros μ_{mn} of the Bessel derivative function $J_m'(\mu)$ as $sR_1 = -i\mu_{mn}$. That is, from (16) we obtain the poles of the function $D_m^{FL}(r, r', k, p)$ in points $p \equiv p_{mn} = -a\left[k^2 + b^2 + (\mu_{mn}/R_1)^2\right]$ $(m = 0, \pm 1, \pm 2, \ldots; n = 1, 2, \ldots)$. Then, returning to the field of originals, after some transformations of

www.czasopisma.pan.pl PAN www.journals.pan.pl

S. Ledakowicz, O. Piddubniak, *Chem. Process Eng.*, 2021, 42 (2), 119–137

this function we receive

$$D_m(r, r', z, \tau) = \frac{1}{R_1^2} \sqrt{\frac{a}{\pi \tau}} \exp\left[-\left(ab^2\tau + \frac{z^2}{4a\tau}\right)\right] \times$$

$$\times \left[\delta_{m0} + \sum_{n=1}^{\infty} \frac{J_m\left(\mu_{mn}\frac{r}{R_1}\right) J_m\left(\mu_{mn}\frac{r'}{R_1}\right)}{\left(1 - \frac{m^2}{\mu_{mn}^2}\right) J_m^2(\mu_{mn})} \exp\left(-\mu_{mn}\frac{a\tau}{R_1^2}\right)\right] \quad (\tau > 0), \tag{24}$$

where δ_{m0} is the Kronecker symbol ($\delta_{00} = 1$; $\delta_{m0} = 0$, $m \neq 0$). Since this function is symmetric with respect to r and r', the integrals over r' in Eq. (23) will pass into one integral over r' from 0 to R_1:

$$U_m(r, z, \tau) = \frac{1}{\lambda R_1^2} \sqrt{\frac{a}{\pi}} \int_0^{R_1} r' \, dr' \int_{-\infty}^{\infty} e^{-b(z-z')} \, dz' \int_0^{\tau} \frac{1}{\sqrt{\tau'}} \exp\left[-\left(ab^2\tau' + \frac{z'^2}{4a\tau'}\right)\right] \times$$

$$\times q_m(r', z - z', \tau') \left[\delta_{m0} + \sum_{n=1}^{\infty} \frac{J_m\left(\mu_{mn}\frac{r}{R_1}\right) J_m\left(\mu_{mn}\frac{r'}{R_1}\right)}{\left(1 - \frac{m^2}{\mu_{mn}^2}\right) J_m^2(\mu_{mn})} \exp\left(-\mu_{mn}\frac{a\tau'}{R_1^2}\right)\right] \quad (\tau > 0) \tag{25}$$

where Eq. (18) is taken into account.

From relation (5), using some properties of the Dirac function and equality (Krein, 1972)

$$\sum_{m=-\infty}^{\infty} \delta(x - 2\pi m) = \frac{1}{2\pi} \sum_{m=-\infty}^{\infty} e^{imx} \tag{26}$$

we obtain

$$q_m(r, z, \tau) = \frac{q_0 \varepsilon}{2\pi \cos\varphi_0 (\varepsilon - \varepsilon_0)} [H(r - R_2) - H(r - R_2)] \times \sum_{m=-\infty}^{\infty} \exp\left[-m(\theta + \omega\tau) - \frac{z}{r}\tan\varphi_0\right] \tag{27}$$

Substituting this function into Eq. (25), after calculating the internal integrals we find

$$U_m(r, z, \tau) = \frac{q_0 \varepsilon e^{-bz} e^{-im\omega\tau}}{\pi \lambda \cos\varphi_0 (\varepsilon - \varepsilon_0)} \left\langle \left\{\frac{1}{2}\left(\varepsilon^2 - \varepsilon_0^2\right) \frac{a\tau}{R_1^2} + R_1^2 \sum_{n=1}^{\infty} \frac{J_0\left(\mu_{0n}\frac{r}{R_1}\right)}{\mu_{0n}^3 J_0^2(\mu_{0n})} \times \right.\right.$$

$$\times \left[\varepsilon J_1(\mu_{0n}\varepsilon) - \varepsilon_0 J_1(\mu_{0n}\varepsilon_0)\right] \left[1 - \exp\left(-\mu_{0n}^2 \frac{a\tau}{R_1^2}\right)\right]\right\} \delta_{m0} +$$

$$+ \sum_{\substack{m=-\infty \\ m \neq 0}}^{\infty} \sum_{n=1}^{\infty} \frac{J_m\left(\mu_{mn}\frac{r}{R_1}\right)}{\left(1 - \frac{m^2}{\mu_{mn}^2}\right) J_m^2(\mu_{mn})} \int_{R_2}^{R_0} \frac{1 - \exp[-\Phi_{mn}(r')]}{a\Phi_{mn}(r')} J_m\left(\mu_{mn}\frac{r'}{R_1}\right) \exp\left(\frac{mz\tan\varphi_0}{r'}\right) r' \, dr' \right\rangle \tag{28}$$

$(\tau > 0)$

where

$$\Phi_{mn}(r') = \mu_{mn}^2 + \left(\frac{mR_1\tan\varphi_0}{r'}\right)^2 + im\left(\frac{2b\tan\varphi_0}{r'} - \frac{\omega}{a}\right) R_1^2 \tag{29}$$

Substituting the function $U_m(r, z, \tau)$ into formula (11) and using the properties (Abramowitz and Stegun, 1972): $J_{-m}(x) = (-1)^m J_m(x)$, $\mu_{-m,n} = \mu_{mn}$, as well as introducing dimensionless variables

$$\xi = \frac{r}{R_1}, \quad \xi' = \frac{r'}{R_1}, \quad \zeta = \frac{z}{R_1}, \quad \text{Fo} = \frac{\alpha\tau}{R_1^2} \tag{30}$$

where Fo is the Fourier number, we obtain the final expression for the temperature in the form

$$
T(r, \theta, z, \tau) \equiv T(\xi, \theta, \zeta, \text{Fo}) = T_0 + \frac{q_0 \varepsilon}{\pi \lambda \cos \varphi_0 (\varepsilon - \varepsilon_0)} \left\langle \left\{ \frac{1}{2} \left(\varepsilon^2 - \varepsilon_0^2 \right) \text{Fo} + \sum_{n=1}^{\infty} \frac{J_0 \left(\mu_{0n} \xi \right)}{\mu_{0n}^3 J_0^2 \left(\mu_{0n} \right)} \times \right. \right.
$$

$$
\times \left[\varepsilon J_1 \left(\mu_{0n} \varepsilon \right) - \varepsilon_0 J_1 \left(\mu_{0n} \varepsilon_0 \right) \right] \left[1 - \exp \left(-\mu_{0n}^2 \text{Fo} \right) \right] \right\} \delta_{m0} +
\tag{31}
$$

$$
+ 2 \sum_{m=1}^{\infty} \sum_{n=1}^{\infty} \frac{J_m \left(\mu_{mn} \xi \right) \Psi_{mn}(\theta, \zeta, \text{Fo})}{\left(1 - m^2/\mu_{mn}^2 \right) J_m^2 (\mu_{mn})} \right\rangle
$$

where

$$
\Psi_{mn}(\theta, \zeta, \text{Fo}) = \int_{\varepsilon_0}^{\varepsilon} \frac{J_m \left(\mu_{mn} \xi' \right)}{A_{mn}(\xi')} \left\{ \cos \left[m \left(\theta - \frac{\zeta \tan \varphi_0}{\xi'} + 2\pi \frac{\text{Fo}}{\text{Fo}_0} \right) + \varphi_{mn}(\xi') \right] \right.
$$

$$
\left. - \cos \left[m \left(\theta - \frac{\zeta \tan \varphi_0}{\xi'} + 2\pi \frac{\text{Fo}}{\xi' \text{Fo}_v} \right) + \varphi_{mn}(\xi') \right] \exp \left[-\frac{\text{Fo}}{\text{Fo}_{mn}(\xi')} \right] \right\} \xi' \, \mathrm{d}\xi'
\tag{32}
$$

$$
A_{mn}(\xi) = \sqrt{ \frac{1}{\text{Fo}_{mn}^2}(\xi) + (2\pi m)^2 \left(\frac{1}{\xi \text{Fo}_v} - \frac{1}{\text{Fo}_0} \right)^2 }
\tag{33}
$$

$$
\varphi_{mn}(\xi) = \arctan \left[2\pi m \text{Fo}_{mn}(\xi) \left(\frac{1}{\xi \text{Fo}_v} - \frac{1}{\text{Fo}_0} \right) \right]
$$

Here Fo_0 is the Fourier number corresponding to the period of screw rotation $\tau_0 = 2\pi/\omega$; $\text{Fo}_0 = \alpha \tau_0 / R_1^2$; Fo_v is the Fourier number corresponding to the period of "rotation" of the biomass particle along the trajectory of the helix on one of the cylindrical surfaces of the screw (e.g., the outer) $\tau_v = 2\pi/\omega_v$, $\omega_v = v_0 \tan \varphi_0 / R_1$; $\text{Fo}_v = \alpha \tau_v / R_1^2$; $\text{Fo}_{mn}(\xi)$ are the Fourier numbers corresponding to the relaxation times of partial heat pulses:

$$
\text{Fo}_{mn}(\xi) = \frac{1}{\mu_{mn}^2 + \left(\dfrac{m \tan \varphi_0}{\xi} \right)^2}
\tag{34}
$$

Note that in the limiting case of small values of the difference $\varepsilon - \varepsilon_0$ ($R_0 - R_2 = R_1$) the formula (31) will correspond to the case of heating biomass in the channel by a screw in the form of a wire with a rectangular cross-sectional area S.

3. NUMERICAL ANALYSIS OF TEMPERATURE DISTRIBUTION

The calculation of the temperature distribution in the channel is performed using thermodynamic (c_p, ρ, λ), thermoelectric (j, ρ_0), geometric (ε, ε_0, φ_0) and kinematic (ω, v_0) parameters. The specific values of these parameters are given below (Nachenius et al., 2015; Shi et al., 2019b):

- initial temperature $T_0 = 293.15$ K,
- outer screw radius $R_0 = 0.025$ m ($\varepsilon = 0.962$),
- inner screw radius $R_2 = 0.009$ m ($\varepsilon_0 = 0.346$),
- thickness of screw $h = 0.003$ m
- channel radius $R_1 = 0.026$ m,
- screw angle $\varphi_0 = 73.68°$ (this corresponds to the pitch of the screw $d = 2\pi R_0 \cot \varphi_0 = 0.046$ m),
- angular velocity of the screw $\omega = 0.292$ Hz (this corresponds to $\text{Fo}_0 = 0.0135$),
- resistivity of the tungsten conductor $\rho_0 = 5.44 \cdot 10^{-8}$ Ω·m,
- heat capacity of the mixture $c_p = 1502$ J/(kg K) at operating temperature $T = 598$ K,

www.czasopisma.pan.pl PAN www.journals.pan.pl

S. Ledakowicz, O. Piddubniak, Chem. Process Eng., 2021, 42 (2), 119–137

- thermal conductivity of the mixture $\lambda = 0.35$ W/(m K),
- density of biomass $\rho = 551$ kg/m^3,
- mass flow rate $v_M = 6.89 \cdot 10^{-4}$ kg/s,
- velocity of the mixture movement $v_0 = v_M / \left(\rho \pi R_1^2 \right) = 5.89 \cdot 10^{-4}$ m/s (this corresponds to Fo$_v$ = 0.593).

The calculations were performed using programs written in the algorithmic language Fortran-90. Herewith, for the calculations of cylindrical functions and zeros μ_{mn}, we use ready-made programs presented by Zhang and Jin (1996). The control over calculation results of these values is carried out on the basis of the tables given by Abramowitz and Stegun (1972). The integral $\Psi_{mn}(\theta, \zeta, \text{Fo})$ is calculated on the basis of Romberg's method (Cheney and Kincaid, 2008).

Fig. 2 shows the time temperature distribution calculated on the axis $\xi = 0$ and on the surface $\xi = 1$ with the above system parameters and $\theta = 0°$, $\zeta = 0.5$, $I = 185$ A (the value of Fo = 0.5 corresponds to $\tau = 13.3$ min). Here, the value for I is set on the basis of the performed temperature measurements $T^* = 1123.15$ K at the specified time $\tau^* = 20$ min (Fo$^* = 0.75$) (Ledakowicz at al., 2019), based on the formula

$$T^* \approx T_0 + \frac{q_0 \varepsilon (\varepsilon + \varepsilon_0)}{2\pi\lambda \cos\varphi_0} \text{Fo}^* \tag{35}$$

that is

$$I \approx \frac{S}{R} \sqrt{\frac{2\pi\lambda \left(T^* - T_0 \right) \cos\varphi_0}{\varepsilon(\varepsilon + \varepsilon_0)\rho_0 \text{Fo}^*}} \tag{36}$$

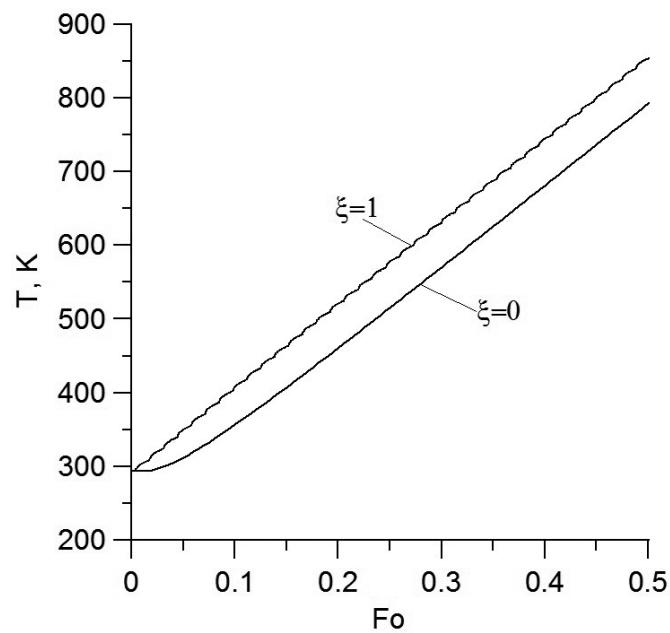
Fig. 2. The time dependence of the temperature at the points $\xi = 0$
and $\xi = 1$, $\theta = 0°$, $\zeta = 0.5$, $I = 185$ A

As can be seen from Fig. 2, the dependence of temperature on time on the axis of the channel is qualitatively the same as in the case, when a constant heat flux is set on the surface of the cylinder (Luikov, 1968), i.e. the temperature is a monotonic function of time. In the classical case (Luikov, 1968), the temperature on the surface of the cylinder is also a monotonic function over time. We have another situation in this study, where the heat source is a rotating screw. Here, the temperature on the surface of the channel is a nonmonotonically increasing and oscillating function of dimensionless time, i.e. the Fourier numbers.

The microstructure of the above time dependence of the temperature on the surface of the channel is shown in Fig. 3. It can be noted that this temperature is an amplitude-modulated function over time (Fig. 3a), and the individual oscillations in shape resemble sawtooth signals with an amplitude of about 18 K (Fig. 3b). The Fourier number corresponding to the period of oscillations (the period of rotation of the screw) is equal to $Fo_0 = 0.0135$.
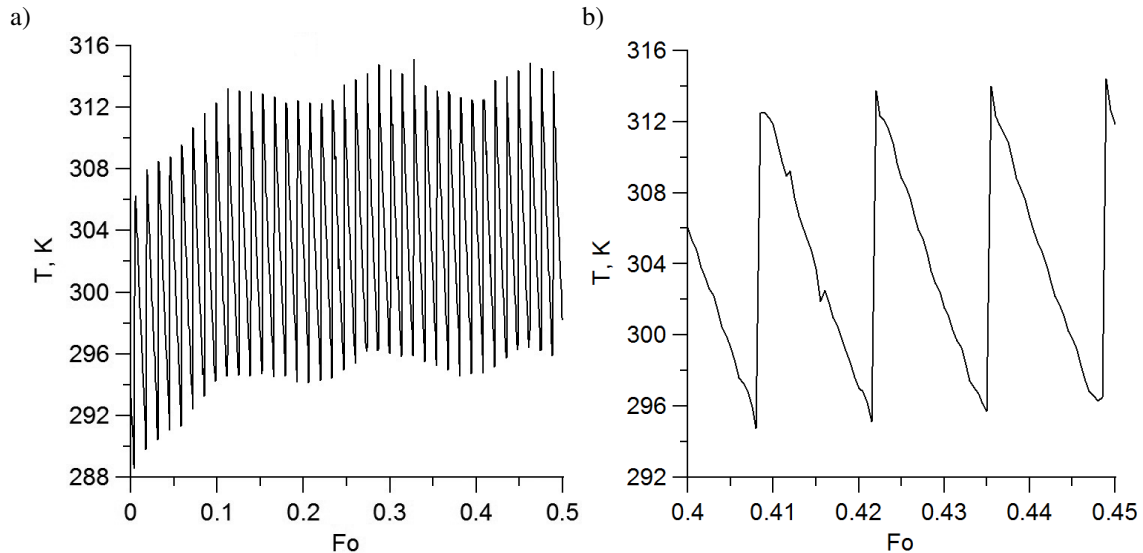

Fig. 3. The time dependence of the temperature T at the point $\xi = 0.8$, $\theta = 0°$, $\zeta = 0.5$, $I = 185$ A without linear term proportional to Fo (a – amplitude-modulated part of the temperature in a wider time range; b – local structure of temperature oscillations)

For a detailed analysis of the thermal state of biomass in the channel, it is advisable to calculate the distribution of temporal characteristics of the temperature in different directions in the channel. In order to be independent of the Joule heat intensity, consider the function $\vartheta = (T - T_0)\pi\lambda/q_0$, which describes the influence of geometry and angular velocity of the screw, as well as thermophysical parameters and flow rate of biomass on the formation of the temperature field. Hereinafter, this function will be called the function of screw influence on the temperature field, or simply the influence function.

Fig. 4 shows the angular-temporal dependence of this function on the circle $\xi = 0.8$, $0 \leq |\theta| \leq 180°$ of the cross-section $\zeta = 0.5$ with constant all other parameters of the system. Here, the range of change of the

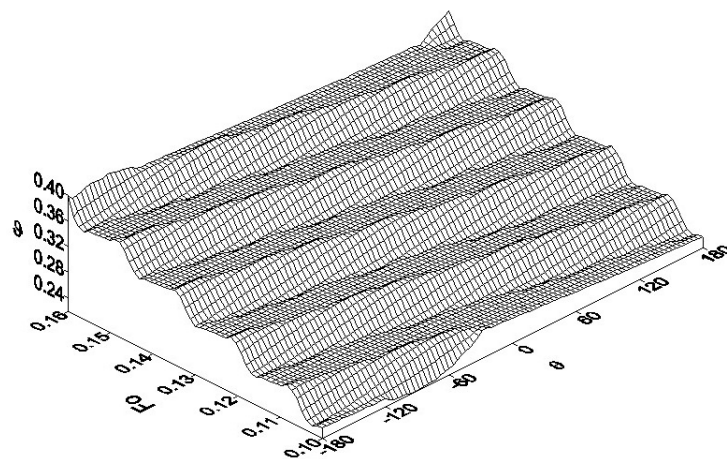Fig. 4. The time dependence of the temperature on the circle $\xi = 0.8$, $0 \leq |\theta| \leq 180°$, $\zeta = 0.5$ for four periods of oscillation

www.czasopisma.pan.pl   PAN   www.journals.pan.pl

S. Ledakowicz, O. Piddubniak, Chem. Process Eng., 2021, 42 (2), 119–137

Fourier number Fo corresponds to four periods of rotation of the screw. In this case $q_0/(\pi\lambda) = 496.8$ K. The calculations show that the function ϑ increases stepwise with time, and the steps are inclined relative to the angular coordinate, and almost unchanged on the plateau surface, i.e. in cross sections of the channel rotated to the axis of symmetry at an angle $\pi/2 - \varphi_0$.

Fig. 5 illustrates the axial-temporal distribution of the influence function ϑ on the generating cylindrical surface $\xi = 0.8$, $\theta = 0°$ along four dimensionless pitchs of the screw $0 \leq |\zeta| < 2\Delta$, $\Delta = d/R_1$ ($d = 2\pi\varepsilon \cot\varphi_0$). As in the previous case, the temperature stepwise increases over time with a dimensionless period Fo_0. Along the axial direction, the temperature also changes periodically. The period of change coincides with the pitch of the screw, within which the temperature amplitude has a sawtooth appearance. In general, the distribution of the temperature field has the character of periodic plateaus, the direction of each of which is inclined at an angle φ_0 to the axis of symmetry of the channel.
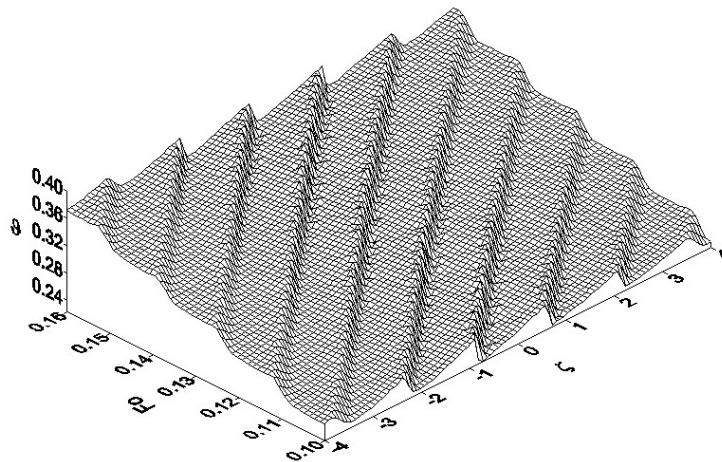

Fig. 5. The time dependence of the function ϑ along the generatrix
of screw cylinder $\xi = 0.8$, $\theta = 0°$

Fig. 6 shows the distribution of the function ϑ on the cross-sectional surface of the channel $\zeta = 0.5$ at time $\tau = 13.3$ min (Fo = 0.5). As can be seen, the temperature increases with the departure from the axis of the channel, and then its value becomes almost constant and even decreases slightly when approaching the surface of the channel. A significant change in temperature in the form of a transition to an elevated plateau is observed in those cross-sections of the channel, where at this time the edge of the screw (in this case at $60° < \theta < 180°$) is situated. It is obvious that with the change of time this plateau transfers its location.
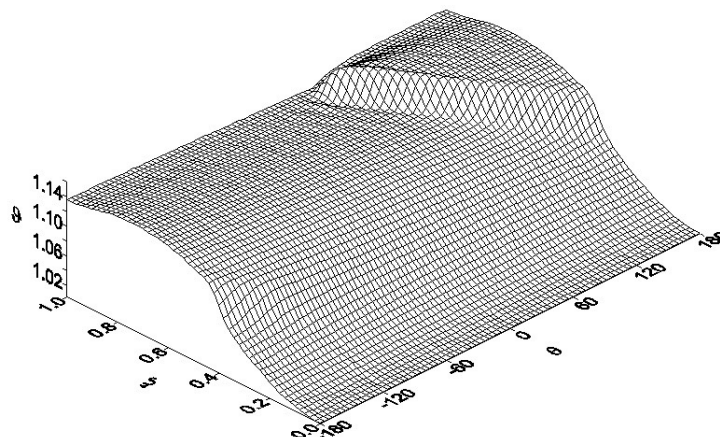

Fig. 6. The three-dimensional radial-angular temperature distribution for $\zeta = 0.5$, Fo = 0.5

Fig. 7 illustrates a similar temperature distribution, but in the plane of the longitudinal section of the channel $\theta = 0°$ within a little more than four steps of the screw $0 \leq |\zeta| \leq 4$ and also at the time when Fo = 0.5. The occurrence of ridges in a profile of a temperature field corresponds to the approach of edges of the screw to points of the plane of this section.
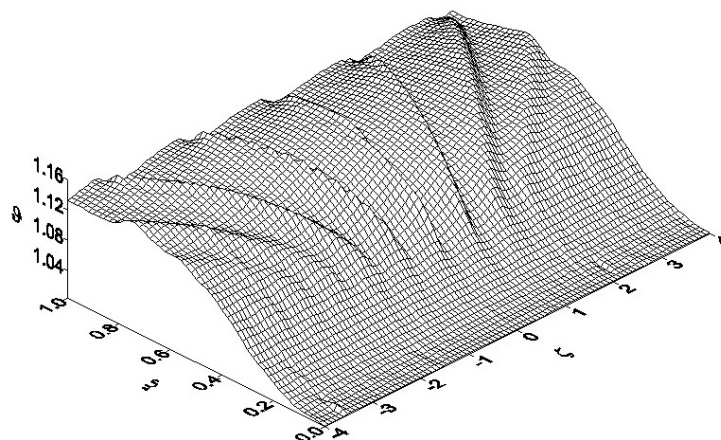

Fig. 7. The instantaneous radial-axial distribution of the function ϑ
in the plane $0 \leq \xi \leq 1, 0 \leq |\zeta| \leq 4$ at $\theta = 0°$, Fo = 0.5

The distribution of the temperature field on the cylindrical surface $\xi = 0.8, 0 \leq |\theta| \leq 180°$ within $0 \leq |\zeta| \leq 4$ inside the channel at Fo = 0.5 is shown in Fig. 8. This figure shows that the temperature profile exactly matches the profile of the screw. In this case, if with the change of the axial coordinate ζ the temperature has a periodic sawtooth character (amplitude of oscillations of the function $\vartheta \approx 0.01$), then in the places of approach of the outer edge of the screw to the cylindrical surface the temperature field on the ridges, inclined to the channel axis at an angle φ_0, is almost constant (within the calculation error).
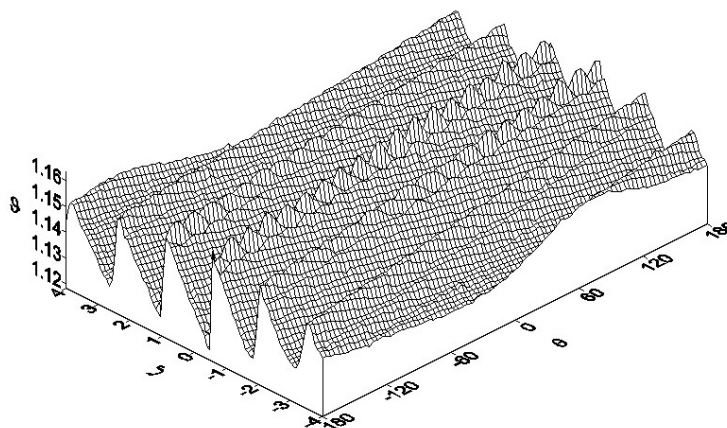

Fig. 8. The instantaneous axial-angular distribution of function ϑ on the surface
of the cylinder $0 \leq |\theta| \leq 180°, 0 \leq |\zeta| \leq 4$ for $\xi = 0.8$, Fo = 0.5

So far, we have investigated the temperature field at constant geometric and kinematic parameters of the system. Let us now evaluate how the temperature changes at a certain point of the channel with a change in the angular velocity and different widths of the screw. It is known that manipulation of the speed of screw rotation allows to flexibly adjust the residence time of the flow of biomass particles inside the screw reactor (Nachenius et al., 2015; Shi et al., 2019b). Therefore, it is important to assess the temperature field that arises.

www.czasopisma.pan.pl   PAN   www.journals.pan.pl

S. Ledakowicz, O. Piddubniak, Chem. Process Eng., 2021, 42 (2), 119–137

Fig. 9 illustrates this case for the influence function ϑ calculated at the point $\xi = 0.8$, $\theta = 0°$, $\zeta = 0.5$, Fo = 0.5 at fixed values of $\varphi_0 = 73.68°$ and $v_0 = 5.89 \cdot 10^{-4}$ m/s. From the calculations it follows that the temperature amplitude varies with the change of the screw speed, decreasing with increasing ω, i.e. the increase in the angular velocity has a damping character.
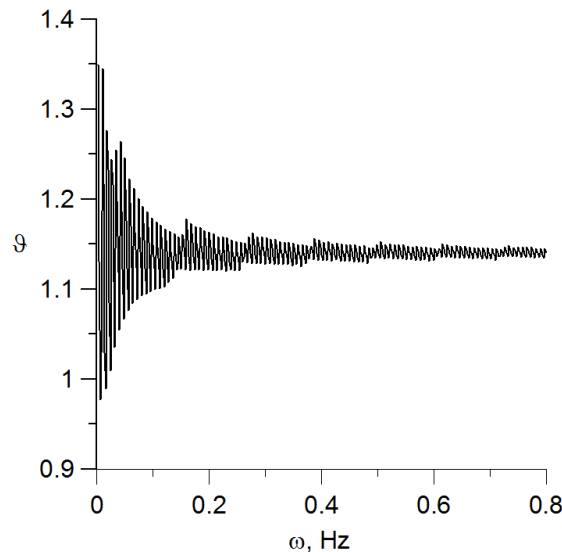

Fig. 9. The dependence of of function ϑ on rotation frequency ω of screw at the point $\xi = 0.8$, $\theta = 0°$, $\zeta = 0.5$, Fo = 0.5 for $\varphi_0 = 73.68°$ and $v_0 = 5.89 \cdot 10^{-4}$ m/s (Fo$_v$ = 0.593)

A similar dependence of the function ϑ can be studied at a fixed angular velocity ω, but at different values of the linear velocity of biomass v_0. However, due to the fact that the chosen value v_0 is very small, and the oscillating term containing this value, according to Eq. (32), is multiplied by the rapidly decaying exponent, it is more advantageous to analyze the dependence of ϑ on the dimensionless Fourier number Fo$_v$. Such characteristic is shown in Fig. 10. It follows that for small values of Fo$_v$ the function ϑ oscillates. However, this range corresponds to large values of the rate v_0, which is unrealistic in the practice of biomass pyrolysis. More realistic is the range of larger values of Fo$_v$, where the function ϑ is almost constant, i.e. the effect of changes in the flow rate of biomass on the temperature field is almost insignificant. In the processing of biomass raw materials with particles of different shapes, sizes and morphological characteristics, the mechanical force from the rotating screw and, consequently, the geometry of the helical shell play an important role (Nachenius et al., 2015; Shi et al., 2019b). Therefore, it is also necessary to monitor how the temperature field changes when the geometric dimensions of the heat source, i.e. the screw, change. The corresponding results of calculations are shown in Fig. 11. In particular, the curve denoted by the letter a illustrates the dependence of the function ϑ on the dimensionless inner radius of the screw ε_0 at a fixed outer radius ($\varepsilon = 0.962$), and the curve denoted by the letter b demonstrates the dependence of this function on the dimensionless outer radius of the screw ε with a fixed inner radius of the screw ($\varepsilon_0 = 0.346$). In both cases, the calculations were performed at the point of the channel $\xi = 0.8$, $\theta = 0°$, $\zeta = 0.5$ for Fo = 0.5, $\omega = 0.292$ Hz, $v_0 = 5.89 \cdot 10^{-4}$ m/s. It is seen that with decreasing screw width the function ϑ increases, but with different behavior of monotonicity.

Fig. 12 illustrates the dynamic effect of "scanning" when a narrow screw of relative width $\Delta_0 = \varepsilon - \varepsilon_0$ moves from the axis of the channel to its surface, with $\varepsilon = \varepsilon_1 + 0.5\Delta_0$, $\varepsilon_0 = \varepsilon_1 - 0.5\Delta_0$.

The calculations are performed for the same point of the channel and with the same kinematic parameters as in the previous figure. From this illustration it is seen that at periodic moments of time when the surface of the screw is near the observation point, the amplitude of the influence function sharply increases. The general trend is that when the screw is placed closer to the surface of the channel, the function ϑ increases.
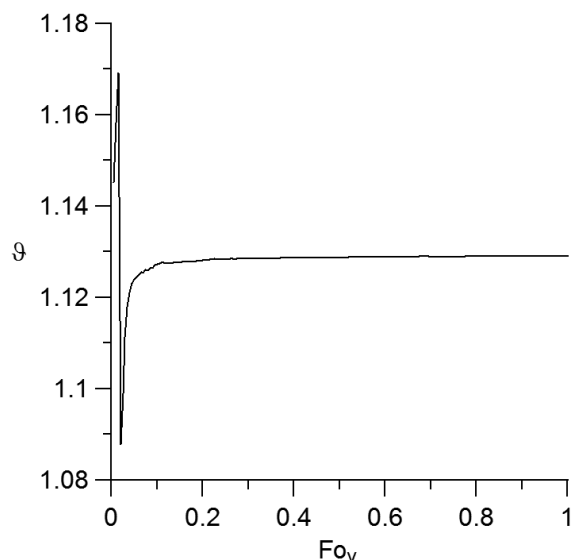
Fig. 10. The dependence of the influence function ϑ on Fourier number Fo_v corresponding to the flow rate of the substance v_0 at the point $\xi = 0.8$, $\theta = 0°$, $\zeta = 0.5$ for $\mathrm{Fo} = 0.5$, $\varphi_0 = 73.68°$, $\omega = 0.292$ Hz ($\mathrm{Fo}_0 = 0.0135$) and $R_2 = 0.009$ m
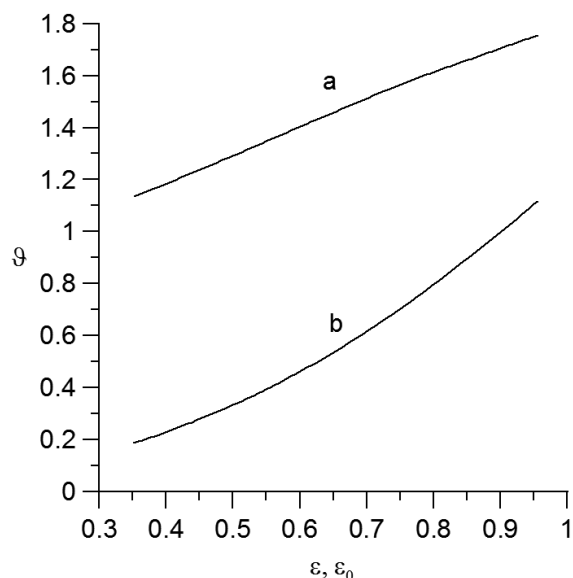

Fig. 11. The dependence of temperature on parameter ε_0 (a) and ε (b) at the point $\xi = 0.8$, $\theta = 0°$, $\zeta = 0.5$ for $\mathrm{Fo} = 0.5$, $\varphi_0 = 73.68°$, $\omega = 0.292$ Hz, $v_0 = 5.89 \cdot 10^{-4}$ m/s

Let us now analyze the influence of the ratio of the pitch and the outer diameter of the screw on the temperature field in the channel. Some practitioners claim that large diameter screws are relatively more efficient to transport than small ones (Henan Pingyuan Mining Machinery, 2015). It has also been found that short-pitch screws feed only a small volume of material per revolution, whereas long-pitch screws tend to rotate the material rather than transfer it in the axial direction (Carleton et al., 1969). Bortolamasi and Fottner (2001) reported that the minimum pitch in the screws should be at least one half of the screw diameter, while the maximum pitch should be approximately equal to one screw diameter. Similarly, Evstratov et al. (2015) concluded that the pitch should not be less than 0.9 and not more than 1.5 times the outer diameter of the screw. Martelli (1983) argues that the ratio of pitch to screw diameter equal to one (known as standard flight) has been also chosen as one of the simplest and optimal options in single-screws and that it is the most common in industrial practice (see also: Carleton et al., 1969; Campuzano et al., 2019). These views on the problem indicate that it is urgent to solve the problem of optimizing the
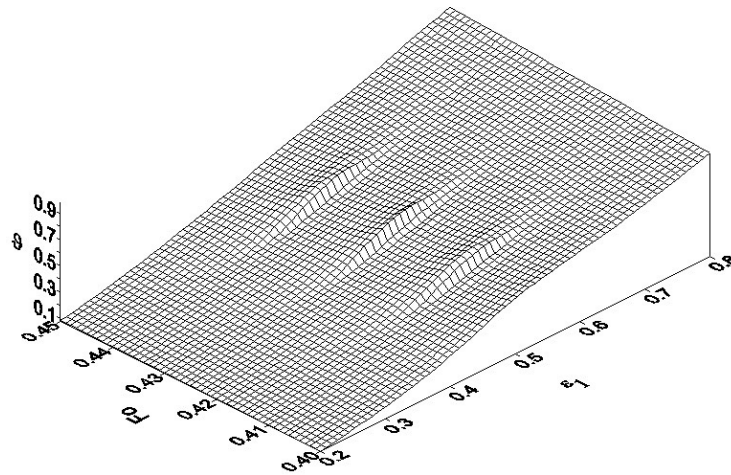
www.czasopisma.pan.pl   PAN   www.journals.pan.pl

S. Ledakowicz, O. Piddubniak, Chem. Process Eng., 2021, 42 (2), 119–137

Fig. 12. The dependence of temperature on parameter ε_1 at the point $\xi = 0.8$, $\theta = 0°$, $\zeta = 0.5$ for $\varphi_0 = 73.68°$, $\omega = 0.292$ Hz, $v_0 = 5.89 \cdot 10^{-4}$ m/s

geometric parameters of the screw in terms of efficiency of the screw system in general. Here we will only illustrate how the change in the screw pitch affects the temperature distribution in the channel.

Fig. 13 shows the change in the influence function ϑ in the axial direction of the channel when changing the angle of rise of the screw. The following parameters and variables are selected here: $\xi = 0.8$, $\theta = 0°$, $0 \leq |\zeta| \leq 4$, Fo $= 0.5$, $\varepsilon = 0.962$, $\varepsilon_0 = 0.346$, $\omega = 0.292$ Hz, $v_0 = 5.89 \cdot 10^{-4}$ m/s. It is obvious that with increasing this angle, the temperature level will increase due to the increase in the number of turns of the screw per running meter of the channel. The convergence of the interference bands, which is observed with increasing φ_0, illustrates the decrease of the screw pitch.
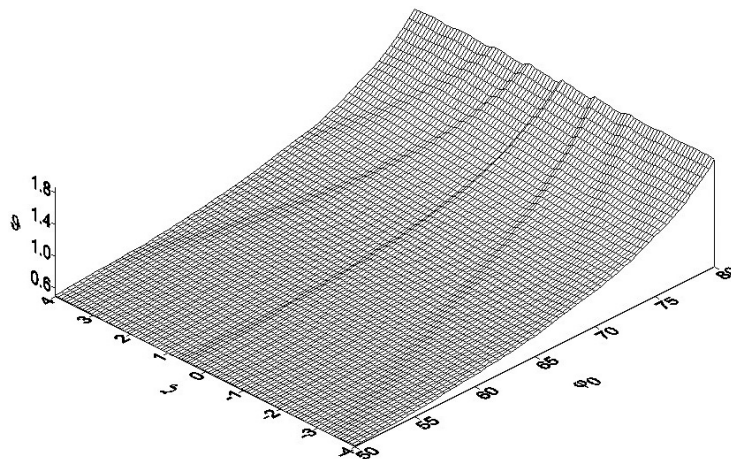

Fig. 13. The instantaneous time (Fo $= 0.5$) dependence of function ϑ along line $\xi = 0.8$, $\theta = 0°$, $0 \leq |\zeta| \leq 4$ on the angle of rise of the screw φ_0

4. CONCLUSIONS

The paper presents an exact solution of the problem of temperature field distribution in a circular thermally insulated channel with mobile homogeneous biomass material under the action of Joule heat, uniformly distributed on the surface of a shaftless rotating screw of finite width. As a result, the temperature field is obtained in the form of the product of the energy source determined by the Joule heat and the influence function, which is represented by the sum of the term proportional to time and the Fourier–Bessel series.

The influence function depends on the thermodynamic characteristics of the substance, its velocity, inner and outer radii and pitch of the screw, and also on angular velocity of screw rotation. Each term of the series contains coefficients in the form of definite integral, which is calculated using the high-precision Romberg method. The performed analytical studies and numerical calculations taking into account the parameters of the systems used in real experiments, allow us to draw the following conclusions.

1. The temperature at all points of the channel is determined by the Joule heat, i.e. the temperature increases in direct proportion to the time of action of the heat source and the coefficient of proportionality depends on the relative outer and inner radii of the screw. However, it should be borne in mind that the density of electric force also depends on these radii. Therefore, changing the size of the screw, the current of the conductor must be adjusted accordingly. Thus, as the radial width of the screw decreases, the power of the current source must be reduced to remain within the correct reactor temperature level for a certain period of time.

2. The temperature field, which is globally determined by the Joule–Lenz effect, is formed locally under the influence of such screw characteristics as angular velocity of rotation, pitch, outer and inner diameters, and also (to a lesser extent) biomass flow rate. The fine structure of the temperature described by the influence function does not depend on the intensity of the Joule heating. Mathematically, this function is described by the superposition of cylindrical harmonics and exponentially attenuating over time pulses, which together are contained under the integral over the dimensionless radial width of the screw.

3. By numerical integration, it was found that due to the non-axisymmetry of the heat source, which is a rotating shaftless screw, the temperature field in the circular channel differs significantly from that known in the classical literature. Thus, in particular, it was found that the temperature on the isolated surface of the channel is not a smooth function, but has an oscillatory character (Fig. 2). A detailed study of the microstructure of the temperature field for a limited period of time showed that this temperature undergoes sinusoidal amplitude-modulated oscillations (Fig. 3a), and these oscillations are sawtooth-shaped (Fig. 3b). The period of oscillations, of course, is determined by the angular angle of rotation of the screw.

4. The study of the influence function at the local level showed that the space-temporal relief of this function largely reflects the geometry of the screw. In particular, the time amplitude is not a monotonically increasing function, but has a stepwise character. The corresponding dependences on the angular (Fig. 4) or axial (Fig. 5) coordinates are depicted as periodically placed plateaus with a slowly varying level. These plateaus are inclined at an angle to the corresponding coordinate lines, which in turn depends on the angle of the screw relative to the axis of symmetry of the channel. The calculated dependences of the influence function on time and radial coordinate showed that the temperature distribution is smooth until the surface of the screw approaches the specified observation point. When the screw directly approaches the observation point, a plateau abruptly appears, on which this function again becomes locally smooth.

5. The calculations of the influence function in the transverse radial-angular section (Fig. 6) and the longitudinal section of the radial-axial (Fig. 7) channel at a fixed time reveal a general trend of temperature increase in the radial direction away from the axis of symmetry of the channel. In this case, the local concentration of the temperature field is related to the closest location of the screw surface to the observation points. The picture changes sharply for the points located on the cylindrical tubes coaxial with the channel surface (Fig. 8). Here the most noticeable screw shape effect occurs. The amplitudes of the temperature field in the axial direction have a sawtooth character and along the surface of such the tubes are placed along the helical trajectories. In the axial direction, the amplitude of the temperature field has a sawtooth character, and its ridges along the surfaces of such tubes, like the edge of the auger, are located along spiral trajectories. Increasing the speed of the screw rotation leads to a general sharp decrease in temperature at a given point (Fig. 9). At the same time, the change

www.czasopisma.pan.pl   PAN   www.journals.pan.pl

S. Ledakowicz, O. Piddubniak, Chem. Process Eng., 2021, 42 (2), 119–137

in the velocity of biomass in the range close to what is practically happening in the screw reactor, does not significantly affect the change in temperature (Fig. 10).

6. The calculations have shown that if the width of the screw decreases, the amplitude of the influence function increases (Fig. 11). In this case, if we perform "scanning" with a narrow screw along the radial direction, then at certain periodic points there will be a burst of the amplitude of the influence function (Fig. 12), which is also explained by the maximum approach of the screw surface to the observation point. As the angle of the screw increases, the pitch of the screw decreases, so, naturally, the temperature level increases. In the axial direction, this it is displayed in the appearance of interference bands, the width of which corresponds to the variable pitch of the screw (Fig. 13).

SYMBOLS

a	thermal diffusivity, $m^2 s^{-1}$
$A_{mn}(\cdot)$	amplitude multipliers
b	constant value, m^{-1}
c_p	material specific heat capacity, $J\,kg^{-1}\,K^{-1}$
d	pitch of screw, m
$D_m(\cdot)$	intermediate function
Fo	Fourier number
Fo*	Fourier number corresponding to time τ^*
Fo_0	Fourier number corresponding to period τ_0
Fo_v	Fourier number corresponding to period τ_v
$Fo_{mn}(\cdot)$	Fourier numbers corresponding to partial heat pulses
h	thickness of screw, m
h_1	width of conductor, m
$H(\cdot)$	Heaviside function
I	force of electric current, A
$I_m(\cdot)$	modified Bessel function of m-th order
j	electric current density of a conductor, $A\,m^{-2}$
$J_m(\cdot)$	Bessel function of m-th order
k	Fourier transform parameter, m^{-1}
$K_m(\cdot)$	McDonald function of the m-th order
m	natural number
n	natural number
p	Laplace transform parameter, s^{-1}
p_0	poles of function, s^{-1}
q_0	heat source intensity, $J\,s^{-1}m^{-1}$
$q(\cdot)$	intensity function of the source, $J\,s^{-1}m^{-1}$
$q_m(\cdot)$	intensity function of the source, $J\,s^{-1}m^{-1}$
$Q_m(\cdot)$	intermediate function
r	radial variable, m
R_0	outer radius of screw, m
R_1	radius of cylindrical channel, m
R_2	inner radius of screw, m
s	variable, m^{-1}
S	cross-sectional area of screw, m^2
$S_m(\cdot)$	intermediate function
$T(\cdot)$	temperature, K

T_0	initial temperature, K
T_*	temperature, K
$U(\cdot)$	auxiliary function, K
$U_m(\cdot)$	auxiliary function, K
v_0	linear velocity of medium, m s^{-1}
v_M	mass flow rate, m s^{-1}
x	variable of Cartesian coordinate system
y	variable of Cartesian coordinate system
z	axial variable, m

Greek symbols

$\delta(\cdot)$	Dirac function
δ_{mn}	Kronecker symbol
ε	dimensionless outer radius of screw
ε_0	dimensionless inner radius of screw
ε_1	additional dimensionless radial coordinate
ζ	dimensionless axial variable
Δ	dimensionless pitch of screw
Δ_0	dimensionless width of screw
θ	angular variable, degree
λ	thermal conductivity, Js^{-1}m^{-1}K^{-1}
μ_{mn}	roots
ξ	dimensionless radial variable
ρ	material density, kg m^{-3}
ρ_0	resistivity of conductor, $\Omega \cdot$m
τ	time, s
τ_0	period of rotation of screw, s
τ_*	exsperimental value of time, min
τ_v	time of passage of pitch distance, s
φ_0	angle of rise of the screw, degree
$\Phi_{mn}(\cdot)$	intermediate function
$\Psi_{mn}(\cdot)$	intermediate function
ω	angular velocity of screw, Hz
ω_v	angular velocity of particle, Hz
$\vartheta(\cdot)$	dimensionless influence function

Subscripts

0	initial, index
F	Fourier transform symbol
L	Laplace transform symbol
m	mode number
M	index
n	mode number
v	index

www.czasopisma.pan.pl   PAN   www.journals.pan.pl

S. Ledakowicz, O. Piddubniak, Chem. Process Eng., 2021, 42 (2), 119–137

REFERENCES

Abramowitz M., Stegun I.A. (Eds), 1972. *Handbook of mathematical functions with formulas, graphs, and mathematical tables*. Dover Publ., Inc., New York.

Aramideh S., Xiong Q., Kong S.C., Brown R.C., 2015. Numerical simulation of biomass fast pyrolysis in an screw reactor. *Fuel*, 156, 234–242. DOI: 10.1016/j.fuel.2015.04.038.

Biogreen, 2016. *The pyrolyzer Spirajoule®*. Available at: https://www.biogreen-energy.com/spirajoule.

Bortolamasi M., Fottner J., 2001. Design and sizing of screw feeders. *PARTEC 2001, International Congress for Particle Technology. Nuremberg*, Germany, 27–29 March 2001.

Campuzano F., Brown R.C., Martínez J.D., 2019. Auger reactors for pyrolysis of biomass and wastes. *Renewable Sustainable Energy Rev.*, 102, 372–409. DOI: 10.1016/j.rser.2018.12.014.

Carleton A.J., Miles J.E.P., Valentin F.H.H., 1969. A study of factors affecting the performance of screw conveyers and feeders. *J. Eng. Ind.*, 91, 329-333. DOI: 10.1115/1.3591565.

Carslaw H.S., Jaeger J.C., 1959. *Conduction of heat in solids*. Clarendon Press, Oxford.

Cheney W., Kincaid D., 2008. *Numerical mathematics and computing*. Thomson Brooks/Cole, Belmont.

ETIA S.A.S., 2019. *Thermal processing of bulk and powders powered by electricity*. Available at: https://etia-group.com/operations-for-thermal-processing.

Evstratov V.A., Rud A.V., Belousov K.Y., 2015. Process modelling vertical screw transport of bulk material flow. *Procedia Eng.*, 129, 397–402. DOI: 10.1016/j.proeng.2015.12.134.

Guda V.K., Steele P.H., Penmetsa V.K., Li Q., 2015. Fast pyrolysis of biomass: Recent advances in fast pyrolysis technology, In: Pandey A., Bhaskar T., Stöcker M., Sukumaran R. (Eds.), *Recent advances in thermochemical conversion of biomass*. Elsevier, Amsterdam etc., 175-211.

Henan Pingyuan Mining Machinery, 2015. *What factors that affect the screw conveyor conveying efficiency?* Available at: https://www.pkmachinery.com/faq/factors–affect–screw-conveyor-conveying-efficiency.html.

Korn G.A., Korn T.U., 2000. *Mathematical handbook for scientists and engineers: Definitions, theorems and formulas for references and review*. Dover Publ., Inc., Mineola, New York.

Kovacevic A., Stosic N., Smith I., 2007. *Screw compressors: Three dimensional computational fluid dynamics and solid fluid interaction*. Springer-Verlag, Heidelberg, Berlin, New York. DOI: 10.1007/978-3-540-36304-0.

Krein S.G. (Ed.), 1972. *Functional analysis*. Wolters-Noorhoff Publ., Groningen.

Ledakowicz S., Stolarek P., Malinowski A., Lepez O., 2019. Thermochemical treatment of sewage sludge by integration of drying and pyrolysis/autogasification. *Renewable Sustainable Energy Rev.*, 104, 319–327. DOI: 10.1016/j.rser.2019.01.018.

Lepez O., Sajet P., 2009. Patent No. WO 2009/095564 A3. *Device for the thermal processing of divided solids*.

Luikov A.V., 1968. *Analytical heat diffusion theory*. Acad. Press, New York etc.

Martelli F.G., 1983. *Twin-screw extruders: A basic understanding*. Van Nostrand Reinhold Co, New York.

Martínez J.D., Murillo R., Garcia T., Veses A., 2013. Demonstration of the waste tire pyrolysis process on pilot scale in a continuous screw reactor. *J. Hazard. Mater.*, 261, 637–645. DOI: 10.1016/j.jhazmat.2013.07.077.

Nachenius R.W., Van De Wardt T.A., Ronsse F., Prins W., 2015. Residence time distributions of coarse biomass particles in a screw conveyor reactor. *Fuel Process Technol*, 130, 87–95. DOI: 10.1016/j.fuproc.2014.09.039.

Shi X., Ronsse F., Roegiers J., Pieters J.G., 2019a. 3D Eulerian-Eulerian modeling of a screw reactor for biomass thermochemical conversion. Part 1: Solids flow dynamics and back-mixing. *Renewable Energy*, 143, 1465-1476. DOI: 10.1016/j.renene.2019.05.098.

Shi X., Ronsse F., Nachenius R., Pieters J.G., 2019b. 3D Eulerian-Eulerian modeling of a screw reactor for biomass thermochemical conversion. Part 2: Slow pyrolysis for char production. *Renewable Energy*, 143, 1477-1487. DOI: 10.1016/j.renene.2019.05.088.

Smirnov V.I., 1964. *A course of higher mathematics, Vol. II: Advanced calculus*. Pergamon Press, Oxford, London, Edinburgh, New York, Paris, Frankfurt. DOI: 10.1016/C2013-0-05341-8.

THERMOFLO Equipment Company, 2018. *Spirajoule®. Revolutionary concept & design in heat exchanger technology*. Available at: https://thermoflotulsa.com/Spirajoule-brochure.pdf.

Yang H., Kudo S., Kuo H.-P., Norinaga K., Mori A., Mašek O., Hayashi J., 2013. Estimation of enthalpy of bio-oil vapor and heat required for pyrolysis of biomass. *Energy Fuels*, 27, 2675–2686. DOI: 10.1021/ef400199z.

Zhang S., Jin J., 1996. *Computation of special functions*. Wiley-Intersci., New York.